

Article

Efficient Removal of Heavy Metal Ions in Wastewater by Using a Novel Alginate-EDTA Hybrid Aerogel

Min Wang^{1,*}, Zhuqing Wang^{1,*}, Xiaohong Zhou¹ and Shikun Li^{2,*}

¹ AnHui Province Key Laboratory of Optoelectronic and Magnetism Functional Materials, College of Chemistry and Chemical Engineering, Anqing Normal University, Anqing 246133, China; wangmin08@aqnu.edu.cn (M.W.); donnelloirgt@gmail.com (X.Z.)

² Institute of Applied and Physical Chemistry, Faculty 2 (Chemistry/Biology), University of Bremen, D-28359 Bremen, Germany

* Correspondence: wangzhq@aqnu.edu.cn (Z.W.); lishikun@uni-bremen.de (S.L.); Tel.: +49-0174-627-7947

Received: 5 January 2019; Accepted: 3 February 2019; Published: 6 February 2019



Abstract: In this study, we prepared a novel calcium alginate-disodium ethylenediaminetetraacetate dihydrate hybrid aerogel (Alg-EDTA) by chemical grafting and vacuum-freeze-drying to remove heavy metal ions from wastewater. Experimental results show that the as-prepared Alg-EDTA adsorbent has a high affinity for heavy metal ions, such as Cd²⁺, Pb²⁺, Cu²⁺, Cr³⁺, and Co²⁺, and can adsorb >85% of metal ions from the corresponding solution. Alg-EDTA also exhibits high selectivity toward Cd²⁺, and the maximum adsorption capacity for Cd²⁺ reached 177.3 mg/g, which exceeds the adsorption capacity of most reported Cd²⁺-adsorbents. Adsorbent regeneration can be achieved by a simple acid-washing process, and adsorption performance of Alg-EDTA remains stable after repeated use. All these findings indicate that Alg-EDTA has a promising prospect in the treatment of heavy metal ions wastewater.

Keywords: heavy metal ions; sorbent; aerogel; sodium alginate

1. Introduction

With the rapid development of industries such as mining, metallurgy, electroplating, and battery manufacture, many heavy metal ions are released into natural waters [1]. These heavy metal ions cannot be biodegraded and can enter and accumulate in the human body through the food chain and drinking water, resulting in a series of irreversible physiological diseases, such as kidney damage, nervous-system disorders, and bone necrosis. Therefore, developing new adsorbent materials for removal of heavy metal ions from wastewater is of great significance [2,3].

Sodium alginate is a byproduct of the extraction of iodine and mannitol from kelp or brown algae (*Sargassum* sp.) and is a natural polysaccharide. Sodium alginate is often used as a food thickener and an antidote for heavy metal poisoning. In our previous research, we have used vacuum-freeze-drying technology and chemical-grafting technology to prepare a series of calcium alginate and modified calcium alginate aerogels [4–7]. These synthesized aerogels provide good selectivity and adsorption capacity for Pb²⁺ ions. The maximum adsorption capacity of the chitosan-modified calcium alginate aerogel for Pb²⁺ ion is up to 468.5 mg/g, which is higher than most of the reported Pb²⁺-adsorbents [5].

Disodium ethylenediaminetetraacetate dihydrate (EDTA) is a good complexing agent with six coordinating atoms (four O and two N atoms), which can coordinate with all metal ions at a 1:1 molar ratio. The content of coordinated metal ions can also be determined by EDTA through complexometric titration [8]. The present study aimed to further improve the adsorption performance and practicability of modified calcium alginate aerogels, which can adsorb various heavy metal ions for treating wastewater containing different types of metal ions. Ethylenediamine was used as a linker

to connect alginate and EDTA, and then the resulting complex was cross-linked with calcium ions in solution. After vacuum-freeze-drying, a novel Alg-EDTA aerogel adsorbent was obtained and used to remove heavy metal ions in wastewater. The composition of the prepared Alg-EDTA adsorbent, as well as its adsorption performance for heavy metal ions and recyclability, were also studied.

2. Materials and Methods

2.1. Materials

Sodium alginate, EDTA salt, metal salts, N-(3-dimethylaminopropyl)-N'-ethylcarbodiimide hydrochloride (EDC), nitric acid (HNO_3), 2-(N-morpholino)ethanesulfonic acid (MES), sodium hydroxide (NaOH), and N-hydroxysuccinimide (NHS) were bought from J&K Scientific Ltd. (Beijing, China). The pH value of the solution was adjusted with 0.05 M HNO_3 or 0.1 M NaOH, and deionized water was used to prepare solutions and wash samples.

2.2. Apparatus

Morphology images of the adsorbent were obtained on an EVO18 scanning electron microscope (SEM, Carl Zeiss GmbH, Dresden, Germany). Infrared (IR) spectra were recorded on a Cary660 Fourier transform IR spectrometer (FTIR, Agilent Technologies Inc., Santa Clara, CA, USA). The metal ion concentrations were measured using an Optima 8000 inductively coupled plasma-optical emission spectrometer (ICP-OES, Perkin-Elmer GmbH, Waltham, MA, USA). X-ray photoelectron spectroscopy analyses were conducted on an Axis-supra X-ray photoelectron spectrometer (XPS, Kratos Analytical Ltd., Manchester, UK).

2.3. Synthesis of the Alg-EDTA

The synthesis route of Alg-EDTA is presented in Figure 1. An appropriate amount of sodium alginate was dissolved in 20 mL of pH 5.5 MES buffer solution, followed by 0.15 g EDC and 0.12 g NHS, after magnetic stirring for 3 h. About 1.5 mL of ethylenediamine was added, and stirring was continued for 6 h, before adding 0.6 g of EDTA salt. After reacting for 6 h, the mixed solution was dropped into 500 mL of 0.2 M $\text{Ca}(\text{NO}_3)_2$ using a 5 mL syringe (Alg-EDTA hydrogel ball formed immediately when the mixed solution contacted with Ca^{2+} solution). The Alg-EDTA hydrogel was separated and washed by ultrapure water three times, then immersed in 40 mL of deionized water, frozen in a $-60\text{ }^\circ\text{C}$ ultra-low temperature freezer for 4 h, and dried in a vacuum-freeze-dryer to finally obtain the Alg-EDTA aerogel.

2.4. Adsorption–Desorption Experiments

Adsorption experiment: Approximately 100 mg of Alg-EDTA was weighed and added to 50 mL 1.5 mM of metal ion solution, magnetically stirred for 6 h and filtered. The residual metal ions in the filtrate was measured using ICP-OES.

Desorption and circulation experiments: Cd^{2+} -loaded or Pb^{2+} -loaded Alg-EDTA was immersed into 50 mL of 0.05 M HNO_3 , magnetically stirred for 6 h, filtered, washed successively with deionized water, calcium hydroxide ($\text{Ca}(\text{OH})_2$), deionized water, and finally dried at $50\text{ }^\circ\text{C}$ for 4 h, thereby obtaining the regenerated Alg-EDTA.

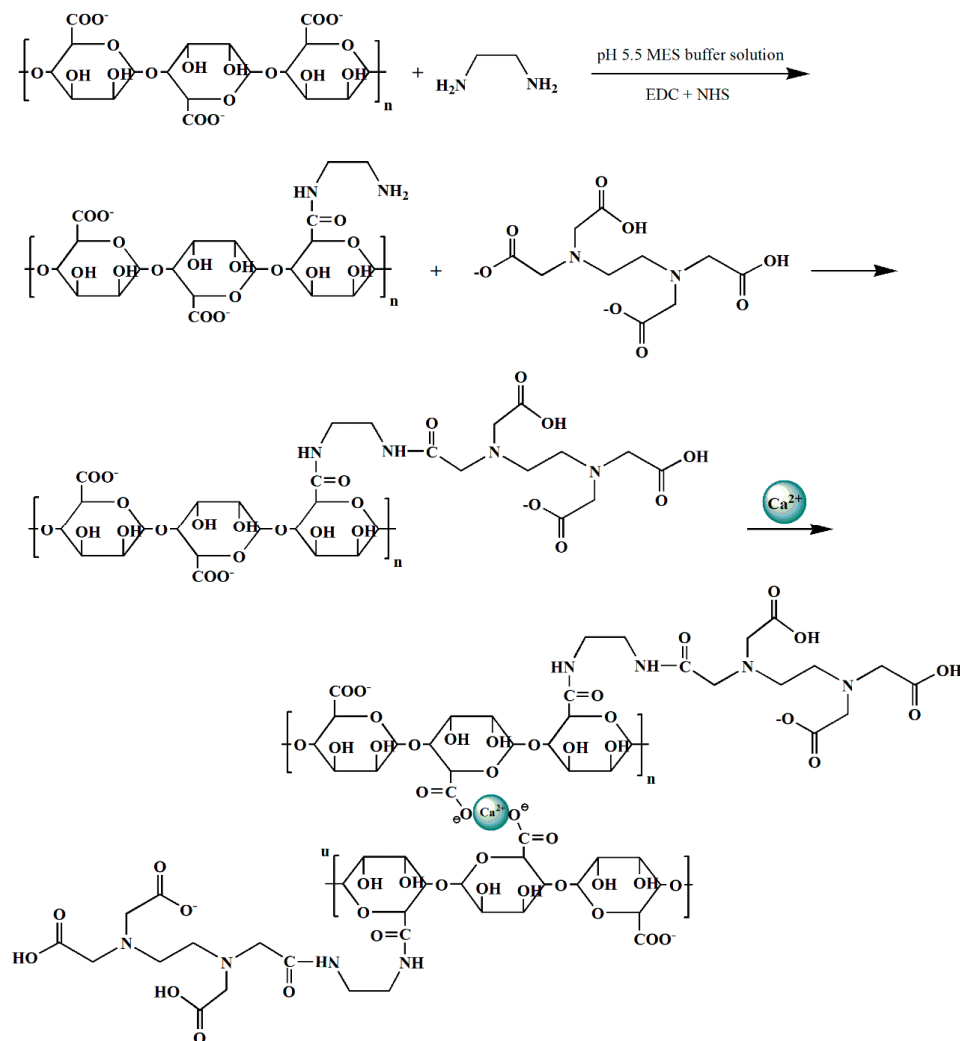


Figure 1. Synthesis route of the calcium alginate-disodium ethylenediaminetetraacetate dihydrate hybrid aerogel (Alg-EDTA).

3. Results and Discussion

3.1. Material Characterization

To confirm whether the EDTA salt was successfully modified to sodium alginate, we determined the IR spectra of sodium alginate, EDTA salt, Alg-EDTA, and Alg-EDTA loaded with Cd^{2+} . As shown in Figure 2, the absorption peaks near 2930 cm^{-1} belong to the aliphatic C-H bond stretching vibration, and the absorption peaks at approximately 1570 and 1310 cm^{-1} can be assigned to the C=O and C-O bond stretching vibrations, respectively [9,10]. The absorption peak of COO^- at 1390 cm^{-1} in the Alg-EDTA was significantly reduced with respect to sodium alginate owing to the condensation reaction of excess amino groups with the COO^- groups [11]. In addition, the absorption peak intensity of C-O bond and C-N bond increases relatively when Alg-EDTA adsorbs Cd^{2+} , which probably results from the coordination of N and O in Alg-EDTA with Cd^{2+} ions.

The morphology of Alg-EDTA has been characterized and illustrated in Figure 3. Similar to one of the lunar surfaces, the surface of Alg-EDTA is rough and porous, which increases the contact area of the adsorbent with the solution and provides more binding sites. In addition, the pore properties of Alg-EDTA were also studied by N_2 adsorption-desorption isotherm (Figure 4). The results showed that the BET surface area, pore volume, and average pore size of Alg-EDTA are $94.63\text{ m}^2/\text{g}$, $53.30\text{ cm}^3/\text{g}$,

and 22.53 nm, respectively. The rough surface and large pore size are beneficial to the rapid adsorption of the target metal ions and the increase in the metal ion adsorption capacity.

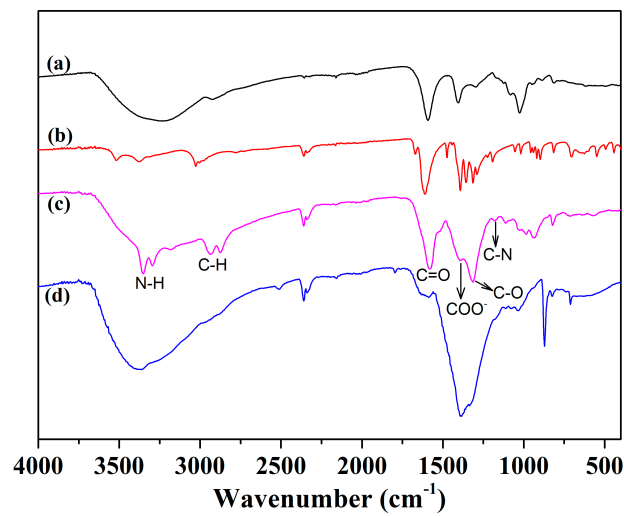


Figure 2. FTIR spectra of (a) sodium alginate, (b) EDTA salt, (c) Alg-EDTA, and (d) Cd²⁺-loaded Alg-EDTA.

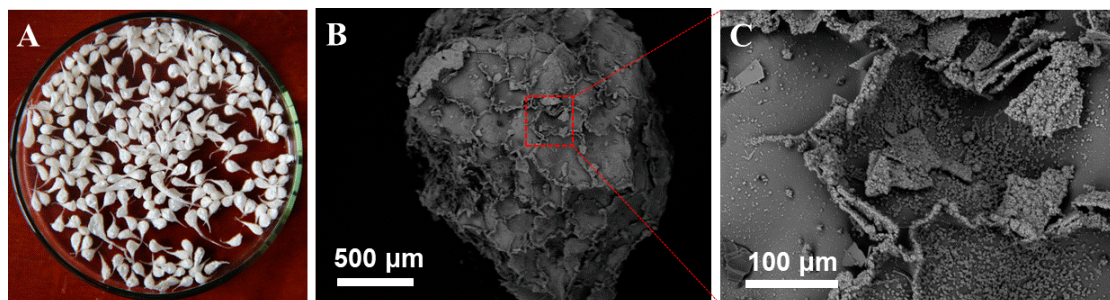


Figure 3. (A) Digital photo of Alg-EDTA; (B) SEM image of Alg-EDTA; (C) partial magnification of (B).

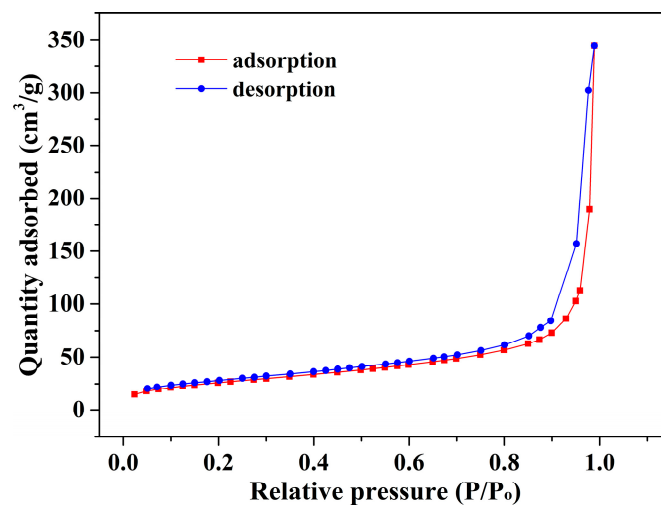


Figure 4. N₂ adsorption-desorption isotherm of the Alg-EDTA.

3.2. Effect of Concentrations of Alginate Sodium

Sodium alginates of 0.5 wt.%, 1.0 wt.% 1.5 wt.%, 2.0 wt.%, and 2.5 wt.% have been selected to prepare Alg-EDTA hybrid aerogel, aiming at evaluating the effect of sodium alginate concentration

on the adsorption performance. The experimental results show that the mechanical properties of the prepared Alg-EDTA aerogel gradually enhance with the increase in the concentration of sodium alginate, and its adsorption capacity for heavy metal ions also gradually increases. An amount of 2.0 wt.% sodium alginate solution was used to prepare the Alg-EDTA adsorbent based on raw material cost, adsorption performance, and ease of operation.

3.3. Effect of pH

Approximately 100 mg of Alg-EDTA was weighed and added to 50 mL of 1.5 mM Cd^{2+} (Pb^{2+} , Cu^{2+} , Cr^{3+} or Co^{2+}) solution of different pH values, stirred for 6 h, and filtered, and the concentration of residual metal ions in the filtrate was determined by ICP-OES. As shown in Figure 5, when the solution pH is less than 1.0, Alg-EDTA can only adsorb 21.3% of Cd^{2+} (19.2% of Pb^{2+} , 17.1% of Cu^{2+} , 14.4% of Cr^{3+} or 13.7% of Co^{2+}) probably due to the protonation of carboxyl and amino groups under strongly acidic conditions, thereby reducing the binding sites of Alg-EDTA with heavy metal ions. With increased solution pH, the adsorption capacity of Alg-EDTA for metal ions increases significantly and then stabilizes. The solubility product rule suggests that Pb^{2+} , Cd^{2+} , Cu^{2+} , Cr^{3+} and Co^{2+} in the solution will separately form the corresponding hydroxide precipitation when the solution pH is higher than 6.5. Therefore, the optimum pH lies in the range of 4.0–6.5 for adsorption of heavy metal ions by Alg-EDTA.

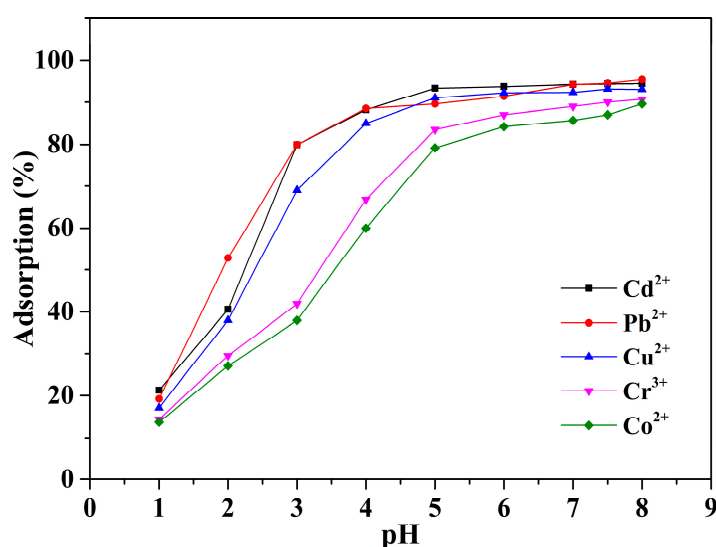


Figure 5. Effect of solution pH on metal ion adsorption of the Alg-EDTA.

3.4. Effect of Adsorption Time

Approximately 100 mg of Alg-EDTA was weighed and added to 50 mL of 1.5 mM Cd^{2+} (Pb^{2+} , Cu^{2+} , Cr^{3+} or Co^{2+}) solution at 25 °C, stirred for 2, 4, 6, 8, 10, 12, 15, 20, 30, 40, 50, 60, ..., 480 or 540 min, and then filtered. The concentration of residual metal ions in the filtrate was determined by ICP-OES. The experimental results are shown in Figure 6. The adsorption capacity of Alg-EDTA for Cd^{2+} and Pb^{2+} increases first, and then remains constant with the increase in the adsorption time. When the adsorption time is 60 min, Alg-EDTA can adsorb more than 40% of heavy metal ions in the solution. While the adsorption time greater than or equal to 360 min, Alg-EDTA can adsorb more than 85% of heavy metal ions in the solution. Therefore, an adsorption time of 360 min was selected in this study. In addition, the pseudo-first-order and pseudo-second-order models were employed to fit the kinetic data in order to study the adsorption mode of metal ions by Alg-EDTA. The fitting results show that the pseudo-first-order and the pseudo-second-order models are fit well with the kinetic data (Table 1), thereby indicating that physisorption and chemisorption are both included in the adsorption mechanism [12,13].

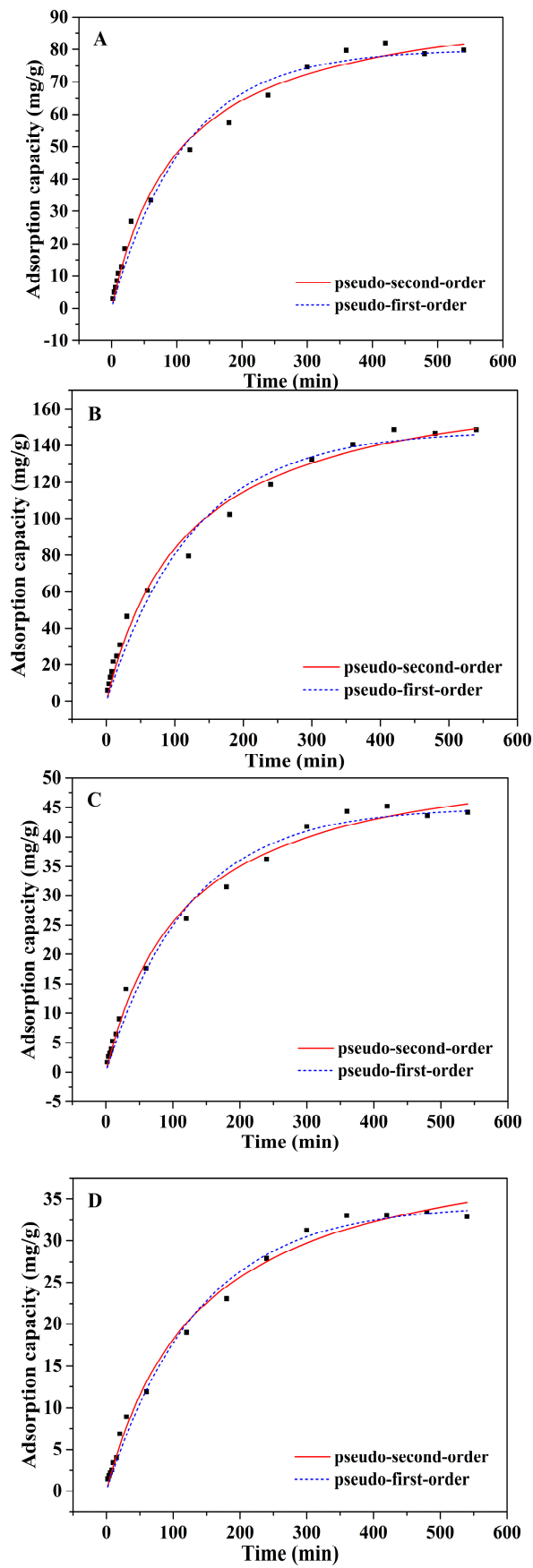


Figure 6. Cont.

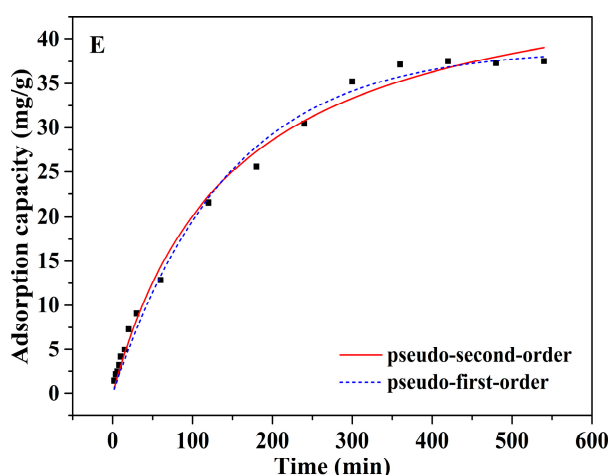


Figure 6. Effect of adsorption time on (A) Cd²⁺, (B) Pb²⁺, (C) Cu²⁺, (D) Cr³⁺ and (E) Co²⁺ sorption by Alg-EDTA.

Table 1. Kinetic parameters for heavy metal ions sorption onto the Alg-EDTA.

Kinetic model	Formula	Parameters	Cd ²⁺	Pb ²⁺	Cu ²⁺	Cr ³⁺	Co ²⁺
pseudo-first-order	$q_t = q_e(1 - \exp(-k_1t))$	q_e (mg/g)	79.932	147.926	44.947	34.328	38.946
		k_1 (L/min)	0.009	0.008	0.008	0.007	0.007
		R ²	0.984	0.979	0.987	0.992	0.992
pseudo-second-order	$q_t = q_e(1 - 1/(1 + q_e k_2 t))$	q_e (mg/g)	97.141	181.306	55.578	43.500	49.693
		k_2 (L/min)	1.006×10^{-4}	4.712×10^{-5}	1.530×10^{-4}	1.651×10^{-4}	1.365×10^{-4}
		R ²	0.991	0.989	0.992	0.993	0.993
-	-	q_e (experiment, mg/g)	82.027	148.56	45.222	33.459	37.526

3.5. Effect of Environmental Temperature

The influence of environmental temperature on the adsorption performance has also been investigated and illustrated in Figure 7. The adsorption performance of the Alg-EDTA is slightly affected by the variance in ambient temperature as shown in the figure. The adsorption rate of Cd²⁺ and Pb²⁺ by Alg-EDTA adsorbents remains between 90–95% in a wide ambient temperature window from 5 °C to 40 °C. Based on these experimental data, the value of Gibbs free energy (ΔG) can be calculated from Equation (1) [14,15], the enthalpy (ΔH) and entropy (ΔS) values can be obtained from the slope and intercept of linear Equation (2), respectively (Figure 8). As listed in Table 2, the negative ΔG at all temperatures indicates that the Alg-EDTA bind to Cd²⁺ spontaneously, the positive ΔH shows that the Cd²⁺ adsorption process is endothermic.

$$\Delta G = -RT \ln K_o \tag{1}$$

$$\ln K_o = \frac{\Delta S}{R} - \frac{\Delta H}{RT} \tag{2}$$

Table 2. Thermodynamic parameters for Cd²⁺ sorption onto Alg-EDTA.

T (K)	ΔG (KJ/mol)	ΔH (KJ/mol)	ΔS (KJ/(mol·K))
288	-2.084	-	-
293	-2.285	-	-
298	-2.507	9.300	0.040
303	-2.668	-	-

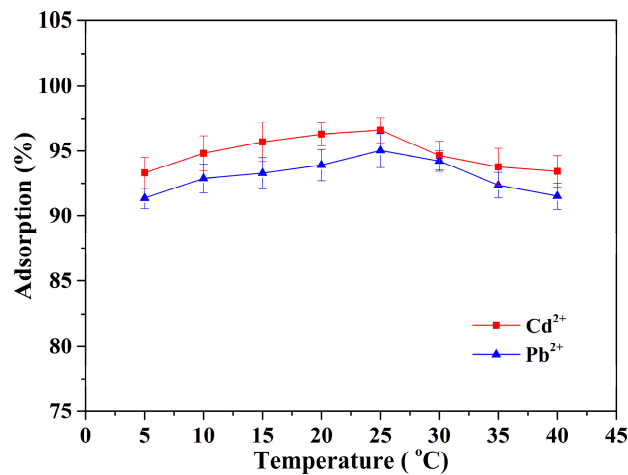


Figure 7. Effect of temperature on metal ion adsorption (100 mg of Alg-EDTA was added to 50 mL 1.5 mM of Cd²⁺ (or Pb²⁺) solution at different temperatures).

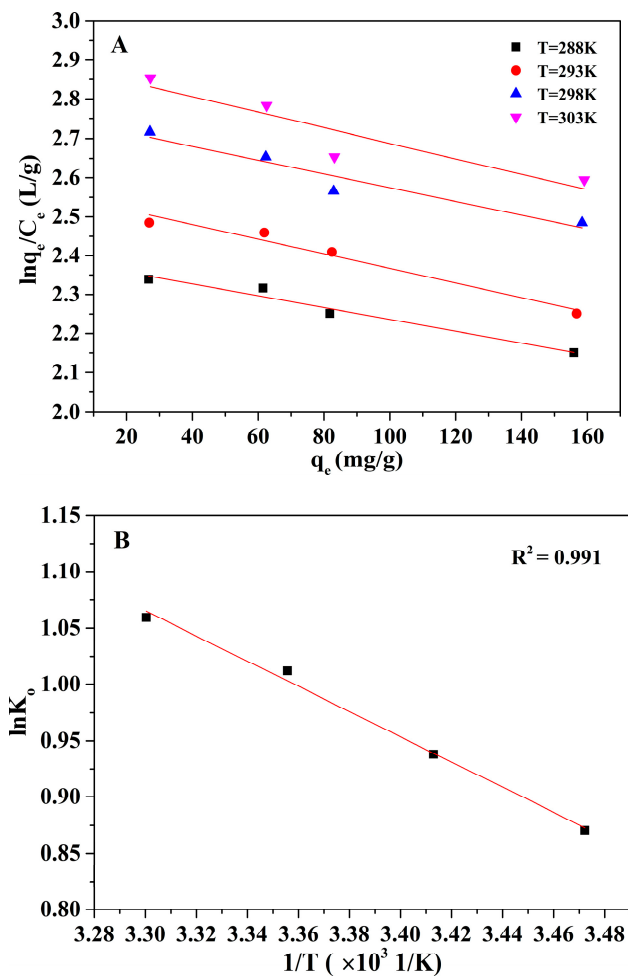


Figure 8. (A) Plots of lnq_e/C_e versus q_e at different temperatures; (B) plot of lnK_o versus 1/T.

3.6. Adsorption Ability and Maximum Adsorption Capacity

To evaluate the adsorption capability of Alg-EDTA for different heavy metal ions, we conducted single metal ion adsorption and competitive adsorption experiments (Table 3). The experimental results show that Alg-EDTA has good affinity for heavy metal ions, such as Cd²⁺, Pb²⁺, Cu²⁺, Co²⁺, and Cr³⁺, and can adsorb more than 80% of the corresponding heavy metal ions in the solution. In competitive

adsorption experiments, Alg-EDTA exhibits higher selectivity for Cd²⁺, it can adsorb more than 90% of Cd²⁺ in the mixed metal ion solution. This may be due to the fact that the ionic radius of Cd²⁺ (0.097 nm) is closer to that of Ca²⁺ (0.100 nm) than Pb²⁺ (0.132 nm) and Cu²⁺ (0.072 nm), and thus has stronger ion exchange effect with Ca²⁺ [16]. We further conducted experiments to determine the maximum adsorption capacity of Alg-EDTA for Cd²⁺, and the experimental results are presented in Figure 9. As the Cd²⁺ concentration in the solution increases from 0.1 mM to 4.0 mM, the adsorption capacity of Alg-EDTA for Cd²⁺ increases rapidly, and then remains stable with further increase in concentration. The maximum adsorption capacity of Alg-EDTA for Cd²⁺ is 177.3 mg/g, which is higher than most of the reported Cd²⁺-sorbents (Table 4) [17–27].

Table 3. The adsorption capacity of Alg-EDTA for heavy metal ions.

Alg-EDTA	Initial concentration (mM)		Adsorption (%)		Adsorption capacity (mg/g)		
In deionized water	1.5 (Cd ²⁺)	-	96.3	-	80.8	-	
	1.5 (Pb ²⁺)	-	95.6	-	157.0	-	
	1.5 (Cu ²⁺)	-	93.8	-	47.1	-	
	1.5 (Zn ²⁺)	-	70.8	-	32.3	-	
	1.5 (Co ²⁺)	-	84.8	-	37.8	-	
	1.5 (Cr ³⁺)	-	85.5	-	33.3	-	
	1.5 (Cd ²⁺)	1.5 (Co ²⁺)	87.0	69.5	73.0	30.8	
	1.5 (Cd ²⁺)	1.5 (Zn ²⁺)	85.9	60.3	72.3	29.5	
	1.5 (Cd ²⁺)	1.5 (Pb ²⁺)	90.4	82.5	76.0	135.5	
	1.5 (Cd ²⁺)	1.5 (Cu ²⁺)	90.2	80.9	75.8	40.5	
	1.5 (Cd ²⁺)	1.5 (Cr ³⁺)	85.1	74.8	71.3	29.3	
	In tap water	1.5 (Cd ²⁺)	-	93.7	-	78.8	-
		1.5 (Cd ²⁺)	1.5 (Pb ²⁺)	91.1	85.5	76.5	140.5
	In pond water	1.5 (Cd ²⁺)	-	91.2	-	76.5	-
1.5 (Cd ²⁺)		1.5 (Pb ²⁺)	90.1	84.2	75.8	138.5	
In river water	1.5 (Cd ²⁺)	-	90.7	-	76.3	-	
	1.5 (Cd ²⁺)	1.5 (Pb ²⁺)	90.1	87.6	75.8	144.0	

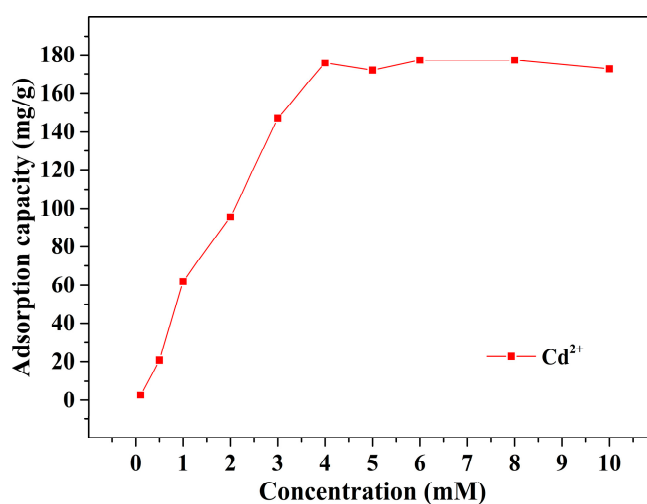


Figure 9. The maximum adsorption capacity of Alg-EDTA for Cd²⁺.

Table 4. The adsorption capacity of different heavy metal ions sorbents for Cd²⁺.

Sorbent	Maximum adsorption capacity for Cd ²⁺ (mg/g)	Adsorption Time (min)	Reference
2-mercaptopyrimidine functionalized Mesoporous silica	112.5	30	[17]
Amino functionalized MCM-41	18.3	120	[18]
Activated carbon-zeolite composite	161.8	1440	[19]
Mango peel waste	68.9	60	[20]
Nano crystallite hydroxyapatite	142	120	[21]
Natural zeolite	130.4	1440	[22]
Clinoptilolite	4.22	2880	[23]
Magnetic modified sugarcane bagasse	123.6	60	[24]
Zeolite synthesized from perlite waste	139.0	1440	[25]
Natural Egyptian bentonitic clay	8.2	60	[26]
L-cystein modified bentonite-cellulose nanocomposite	16.1	2880	[27]
Alg-EDTA	177.3	360	This study

3.7. Adsorption Mechanism

The variation tendency of the concentration of metal ions in the solution has also been monitored during the adsorption process in order to clarify the adsorption mechanism of the Alg-EDTA. It turns out that the amount of Pb²⁺ (or Cd²⁺) in the solution gradually decreases in the progress of adsorption, whereas the amount of Ca²⁺ gradually increases due to the ion exchange effect between Ca²⁺ in Alg-EDTA and Pb²⁺ (or Cd²⁺) in solution. However, after adsorption, the amount of Ca²⁺ released from Alg-EDTA (0.041 ± 0.002 mmol) is evidently smaller than the amount of adsorbed Pb²⁺ or Cd²⁺ (0.072 ± 0.002 mmol), the ion exchange effect contributes approximately 56.9% of metal ions adsorption. It indicates that ion exchange effect is not the only approach in which Alg-EDTA binds to Pb²⁺ (or Cd²⁺) ions. Therefore, we analyzed the XPS spectra of Alg-EDTA before and after adsorption. As shown in Figure 10A, the new Pb 4f and Pb 5s peaks for Alg-EDTA loaded Pb²⁺ verify that Alg-EDTA successfully loaded Pb²⁺ after equilibrated with Pb²⁺-containing solution. The binding energy of the O element of Alg-EDTA shifts from 529.86 to 529.07 eV, it might be caused by the coordination effect between O atoms in Alg-EDTA with Pb²⁺ ions [28]. Based on IR, XPS, and heavy metal ions concentration analysis of the Alg-EDTA sorbent before and after adsorption, we proposed a possible adsorption mechanism of the Alg-EDTA combines with heavy metal ions as depicted in Figure 11.

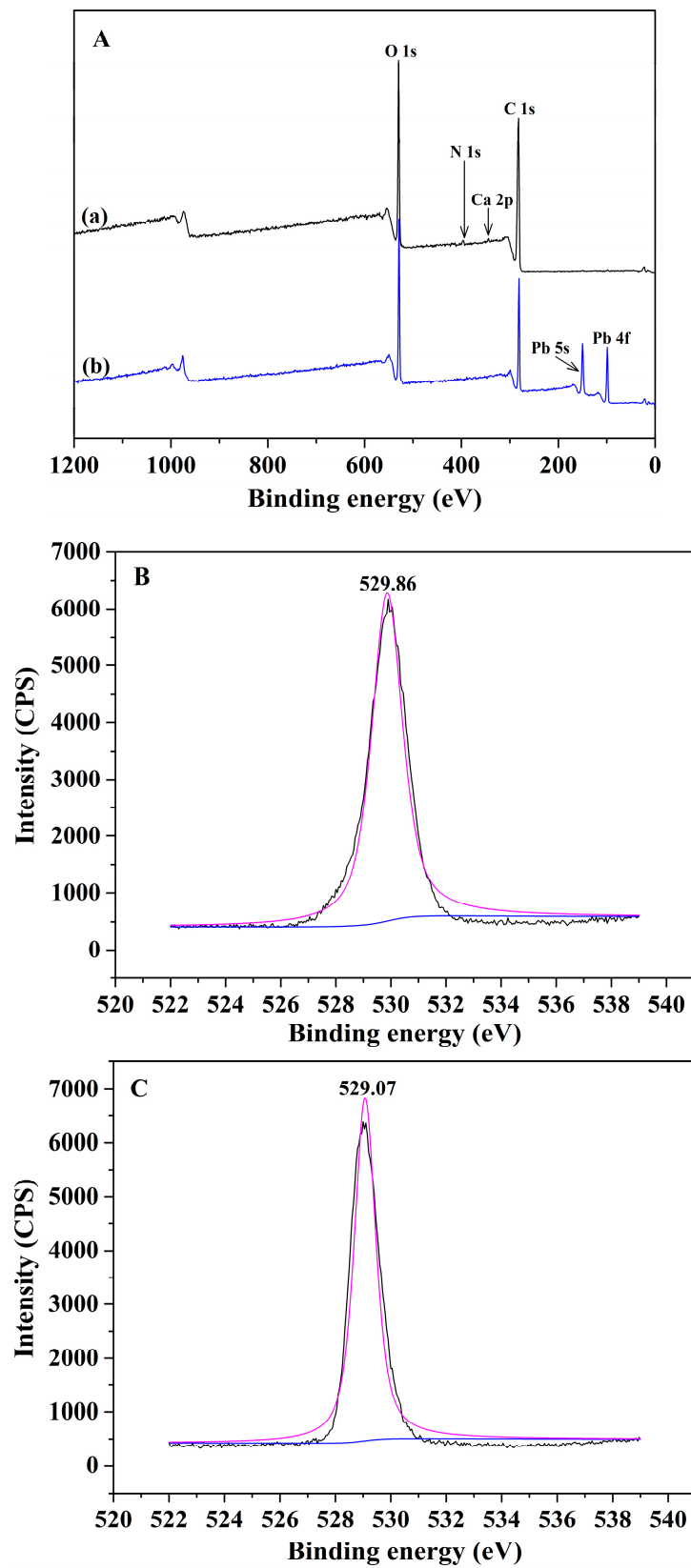


Figure 10. (A) XPS survey of (a) Alg-EDTA and (b) Alg-EDTA loaded Pb²⁺. O 1s spectra of Alg-EDTA (B) before and (C) after Pb²⁺ adsorption.

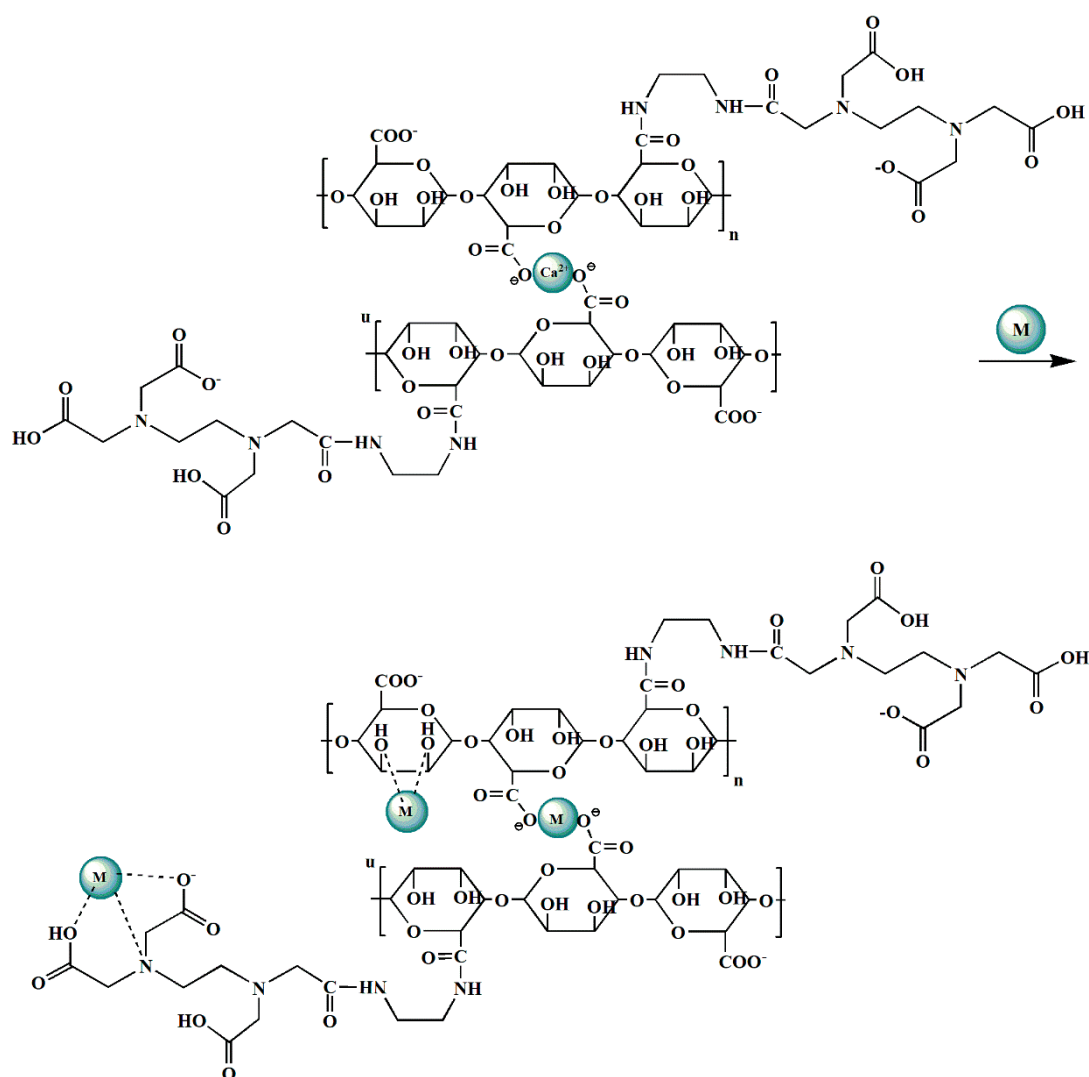


Figure 11. Plausible adsorption mechanism of Alg-EDTA combined with heavy metal ions. M represents heavy metal ions such as Cd²⁺, Pb²⁺, Cu²⁺, etc.

3.8. Regeneration Performance

H protons can exchange metal ions attached to the carboxyl group and the amino group by protonation under acidic conditions. Therefore, we use 0.05 M HNO₃ as an eluent to elute the Cd²⁺-loaded Alg-EDTA to achieve regeneration of the adsorbent. As shown in Figure 12, the adsorption rate of Alg-EDTA to Cd²⁺ still lies in the range of 92.0–95.0% after nine adsorption–desorption cycles, although the morphology of Alg-EDTA changed slightly (from spherical to flat). We propose that the as-prepared Alg-EDTA has stable adsorption performance after the repetition of the usage acting as a potential low-cost and highly-efficient heavy metal ion adsorbent. Moreover, we further analyzed the chemical composition of the Alg-EDTA using an elemental analyzer. Elemental analysis result shows that the C%, N% and H% of initial Alg-EDTA is 35.27%, 15.21% and 3.84%, respectively. The C%, N% and H% of Alg-EDTA after nine adsorption-desorption cycles is 34.36%, 14.47% and 4.05%, respectively. The chemical composition of Alg-EDTA after repeated use is consistent with that before adsorption.

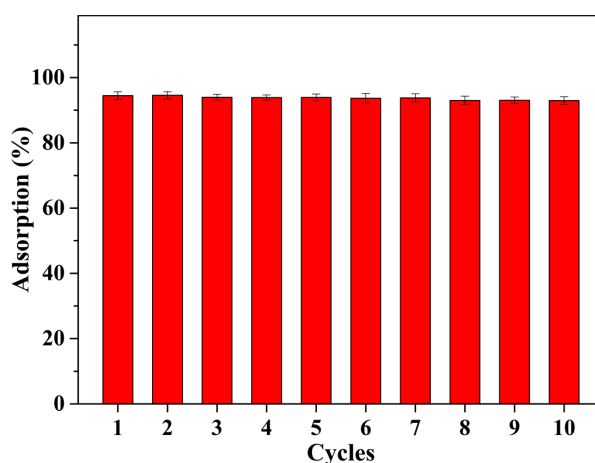


Figure 12. Adsorption performance of the Alg-EDTA in nine adsorption–desorption cycles.

4. Conclusions

In this study, a novel heavy metal ions adsorbent (Alg-EDTA) was successfully prepared by grafting EDTA salt onto sodium alginate. Owing to the strong coordination ability of EDTA and ion exchange effect of Ca^{2+} with heavy metal ions, the as-prepared Alg-EDTA shows high affinity for heavy metal ions such as Cd^{2+} , Pb^{2+} , Cu^{2+} , Cr^{3+} , and Co^{2+} . The maximum adsorption capacity of Alg-EDTA for Cd^{2+} is up to 177.3 mg/g, which is higher than most of the reported Cd^{2+} -sorbents. Alg-EDTA has shown potential applications in the treatment of heavy metal ion wastewater by virtue of the low-cost raw materials, simple synthesis and regeneration processes, and recyclability.

Author Contributions: Conceptualization, Z.W.; formal analysis, X.Z.; investigation, M.W.; writing—original draft preparation, Z.W. and M.W.; writing—review and editing, Z.W. and S.L.

Funding: This work was supported by the natural science foundation of Anhui province grant number [No. KJ2017A345].

Conflicts of Interest: The authors declare no conflict of interest.

References

- Babel, S.; Kurniawan, T.A. Low-cost adsorbents for heavy metals uptake from contaminated water: A review. *J. Hazard. Mater.* **2003**, *97*, 219–243. [[CrossRef](#)]
- Fu, F.L.; Wang, Q. Removal of heavy metal ions from wastewaters: A review. *J. Environ. Manag.* **2011**, *92*, 407–418. [[CrossRef](#)] [[PubMed](#)]
- Jia, T.; Guo, T.Y.; Cao, M.W.; Chai, B.F. Effects of heavy metals on phyllosphere and rhizosphere microbial community of bothriochloa ischaemum. *Appl. Sci.* **2018**, *8*, 1419. [[CrossRef](#)]
- Wang, Z.Q.; Huang, Y.G.; Wang, M.; Wu, G.H.; Geng, T.M.; Zhao, Y.G.; Wu, A.G. Macroporous calcium alginate aerogel as sorbent for Pb^{2+} removal from water media. *J. Environ. Chem. Eng.* **2016**, *4*, 3185–3192. [[CrossRef](#)]
- Wang, Z.Q.; Jin, P.X.; Wang, M.; Wu, G.H.; Sun, J.Y.; Zhang, Y.J.; Dong, C.; Wu, A.G. Highly efficient removal of toxic Pb^{2+} from wastewater by an alginate-chitosan hybrid adsorbent. *J. Chem. Technol. Biotechnol.* **2018**, *93*, 2691–2700. [[CrossRef](#)]
- Wang, Z.Q.; Wu, A.G.; Ciacchi, L.C.; Wei, G. Recent advances in nanoporous membranes for water purification. *Nanomaterials* **2018**, *8*, 65. [[CrossRef](#)] [[PubMed](#)]
- Huang, Y.G.; Wang, Z.Q. Preparation of composite aerogels based on sodium alginate, and its application in removal of Pb^{2+} and Cu^{2+} from water. *Int. J. Biol. Macromol.* **2018**, *107*, 741–747. [[CrossRef](#)]
- Dabrowski, A.; Hubicki, Z.; Podkoscielny, P.; Robens, E. Selective removal of the heavy metal ions from waters and industrial wastewaters by ion-exchange method. *Chemosphere* **2004**, *56*, 91–106. [[CrossRef](#)]
- Ziaei, E.; Mehdinia, A.; Jabbari, A. A novel hierarchical nanobiocomposite of graphene oxide-magnetic chitosan grafted with mercapto as a solid phase extraction sorbent for the determination of mercury ions in environmental water samples. *Anal. Chim. Acta* **2014**, *850*, 49–56. [[CrossRef](#)]

10. Kang, J.Y.; Zhang, Y.J.; Li, X.; Miao, L.J.; Wu, A.G. A rapid colorimetric sensor of clenbuterol based on cysteamine-modified gold nanoparticles. *ACS Appl. Mater. Interfaces* **2016**, *8*, 1–5. [[CrossRef](#)]
11. Perez, M.R.; Pavlovic, I.; Barriga, C.; Cornejo, J.; Hermosin, M.C.; Ulibari, M.A. Uptake of Cu²⁺, Cd²⁺ and Pb²⁺ on Zn-Al layered double hydroxide intercalated with edta. *Appl. Clay Sci.* **2006**, *32*, 245–251. [[CrossRef](#)]
12. Deze, E.G.; Papageorgiou, S.K.; Favvas, E.P.; Katsaros, F.K. Porous alginate aerogel beads for effective and rapid heavy metal sorption from aqueous solutions: Effect of porosity in Cu²⁺ and Cd²⁺ ion sorption. *Chem. Eng. J.* **2012**, *209*, 537–546. [[CrossRef](#)]
13. Pradhan, N.; Rene, E.R.; Lens, P.N.L.; Dipasquale, L.; D'Ippolito, G.; Fontana, A.; Panico, A.; Esposito, G. Adsorption behaviour of lactic acid on granular activated carbon and anionic resins: Thermodynamics, isotherms and kinetic studies. *Energies* **2017**, *10*, 665. [[CrossRef](#)]
14. Xi, J.H.; He, M.C.; Lin, C.Y. Adsorption of antimony(III) and antimony(V) on bentonite: Kinetics, thermodynamics and anion competition. *Microchem. J.* **2011**, *97*, 85–91. [[CrossRef](#)]
15. Yang, X.Z.; Zhou, T.Z.; Ren, B.Z.; Hursthouse, A.; Zhang, Y.Z. Removal of Mn(II) by sodium alginate/graphene oxide composite double-network hydrogel beads from aqueous solutions. *Sci. Rep.* **2018**, *8*, 10717. [[CrossRef](#)] [[PubMed](#)]
16. Tansel, B.; Sager, J.; Rector, T.; Garland, J.; Strayer, R.F.; Levine, L.F.; Roberts, M.; Hummerick, M.; Bauer, J. Significance of hydrated radius and hydration shells on ionic permeability during nanofiltration in dead end and cross flow modes. *Sep. Purif. Technol.* **2006**, *51*, 40–47. [[CrossRef](#)]
17. Perez-Quintanilla, D.; del Hierro, I.; Fajardo, M.; Sierra, I. Adsorption of cadmium(II) from aqueous media onto a mesoporous silica chemically modified with 2-mercaptopyrimidine. *J. Mater. Chem.* **2006**, *16*, 1757–1764. [[CrossRef](#)]
18. Heidari, A.; Younesi, H.; Mehraban, Z. Removal of Ni(II), Cd(II), and Pb(II) from a ternary aqueous solution by amino functionalized mesoporous and nano mesoporous silica. *Chem. Eng. J.* **2009**, *153*, 70–79. [[CrossRef](#)]
19. Jha, V.K.; Matsuda, M.; Miyake, M. Sorption properties of the activated carbon-zeolite composite prepared from coal fly ash for Ni²⁺, Cu²⁺, Cd²⁺ and Pb²⁺. *J. Hazard. Mater.* **2008**, *160*, 148–153. [[CrossRef](#)]
20. Iqbal, M.; Saeed, A.; Zafar, S.I. FTIR spectrophotometry, kinetics and adsorption isotherms modeling, ion exchange, and edx analysis for understanding the mechanism of Cd²⁺ and Pb²⁺ removal by mango peel waste. *J. Hazard. Mater.* **2009**, *164*, 161–171. [[CrossRef](#)]
21. Mobasherpour, I.; Salahi, E.; Pazouki, M. Comparative of the removal of Pb²⁺, Cd²⁺ and Ni²⁺ by nano crystallite hydroxyapatite from aqueous solutions: Adsorption isotherm study. *Arab. J. Chem.* **2012**, *5*, 439–446. [[CrossRef](#)]
22. Castaldi, P.; Santona, L.; Enzo, S.; Melis, P. Sorption processes and XRD analysis of a natural zeolite exchanged with Pb²⁺, Cd²⁺ and Zn²⁺ cations. *J. Hazard. Mater.* **2008**, *156*, 428–434. [[CrossRef](#)] [[PubMed](#)]
23. Sprynskyy, M.; Buszewski, B.; Terzyk, A.P.; Namiesnik, J. Study of the selection mechanism of heavy metal (Pb²⁺, Cu²⁺, Ni²⁺, and Cd²⁺) adsorption on clinoptilolite. *J. Colloid Interfaces Sci.* **2006**, *304*, 21–28. [[CrossRef](#)] [[PubMed](#)]
24. Yu, J.X.; Wang, L.Y.; Chi, R.A.; Zhang, Y.F.; Xu, Z.G.; Guo, J. Competitive adsorption of Pb²⁺ and Cd²⁺ on magnetic modified sugarcane bagasse prepared by two simple steps. *Appl. Surf. Sci.* **2013**, *268*, 163–170. [[CrossRef](#)]
25. Krol, M.; Matras, E.; Mozgawa, W. Sorption of Cd²⁺ ions onto zeolite synthesized from perlite waste. *Int. J. Environ. Sci. Technol.* **2016**, *13*, 2697–2704. [[CrossRef](#)]
26. Burham, N.; Sayed, M. Adsorption behavior of Cd²⁺ and Zn²⁺ onto natural egyptian bentonitic clay. *Minerals* **2016**, *6*, 129. [[CrossRef](#)]
27. Ahmad, R.; Hasan, I. L-cystein modified bentonite-cellulose nanocomposite (cellu/cys-bent) for adsorption of Cu²⁺, Pb²⁺, and Cd²⁺ ions from aqueous solution. *Sep. Sci. Technol.* **2016**, *51*, 381–394. [[CrossRef](#)]
28. Liu, Y.; Lou, Z.M.; Sun, Y.; Zhou, X.X.; Baig, S.A.; Xu, X.H. Influence of complexing agent on the removal of Pb(II) from aqueous solutions by modified mesoporous SiO₂. *Microporous Mesoporous Mater.* **2017**, *246*, 1–13. [[CrossRef](#)]

